

Aromatic long chain cations of amphiphilic ionic liquids permeabilise the inner mitochondrial membrane and induce mitochondrial dysfunction at cytotoxic concentrations

Meryem-Nur Duman¹, Alexander Angeloski^{1,2}, Michael S. Johnson^{3,4}, Tristan Rawling^{1*}

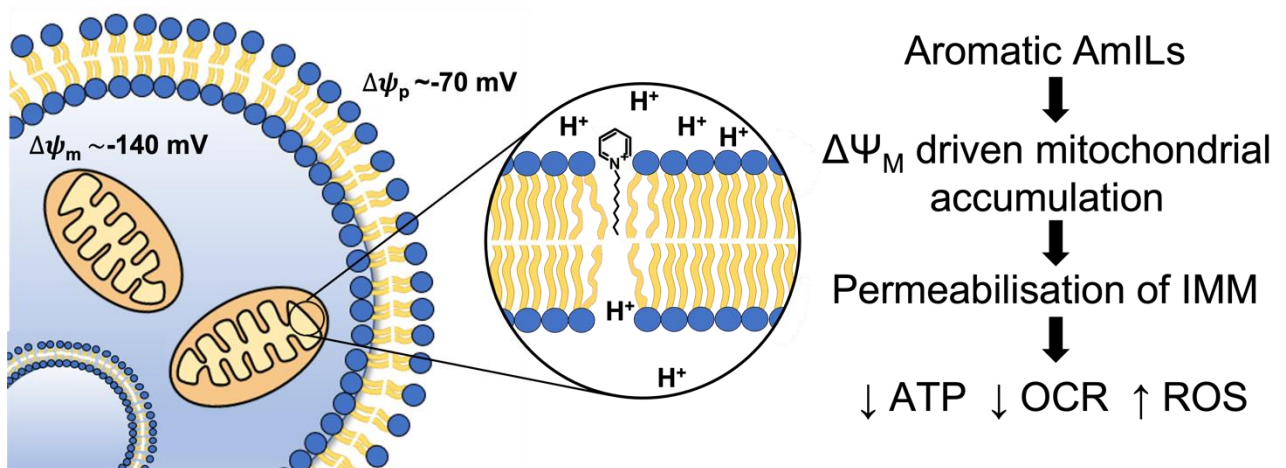
¹School of Mathematical and Physical Sciences, Faculty of Science, University of Technology Sydney, Sydney, NSW, 2007, Australia;

²National deuteration facility, Australia Nuclear Science and Technology Organisation, Lucas Heights, Sydney, NSW, 2232, Australia;

³School of Life Sciences, Faculty of Science, University of Technology Sydney, Sydney, NSW, 2007, Australia;

⁴School of Biomedical Sciences, Faculty of Medicine, University of New South Wales, Sydney, NSW, 2052, Australia;

Graphical Abstract Figure



Abstract

Understanding the cellular mechanisms by which amphiphilic ionic liquids (AmILs) induce cytotoxicity is an important step in the development of task specific AmILs for safe industrial application or as cytotoxic anticancer agents. Accumulated evidence suggests that AmILs kill cells by disrupting cellular membranes and/or inducing mitochondrial dysfunction. The cation of AmILs is lipophilic due to alkyl substitution, and lipophilic cations are a group of compounds known to accumulate in mitochondria in response to the membrane potential across the inner mitochondrial membrane (IMM). We therefore hypothesized that AmILs exert their cytotoxic effects by disrupting the IMM, the integrity of which is critical to several important cellular processes. Using fluorescence microscopy we show that a quinolinium-based AmILs rapidly accumulates in the mitochondria of HeLa cells. In a panel of AmILs we found that cytotoxicity correlates their capacity to disrupt lipid bilayers, and that AmILs produce a range of cellular effects consistent with permeabilisation of the IMM at cytotoxic concentrations. Thus, AmILs depolarise IMM, inhibit oxidative phosphorylation and ATP synthesis, and induce ROS formation. These effects were only induced by AmILs with aromatic cations substituted with long (decyl) alkyl chains, as these features promote accumulation in, and permeabilisation of, the IMM. These mechanistic insights help explain the structure-activity relationship governing AmILs cytotoxicity and may be used to rationally design either safe or cytotoxic AmILs.

Introduction

Amphiphilic ionic liquids (AmILs) are low melting point ionic compounds that contain an alkyl-substituted organic cation and inorganic anion (Figure 1). The physicochemical properties of AmILs can be readily controlled through different combinations of cations and anions which have allowed for the development of task-specific AmILs with potential applications as solvents and catalysts in areas such as food processing, battery and energy research, and pharmaceuticals.¹⁻⁵ AmILs were initially considered environmentally friendly safe solvents due to their low flammability and vapour pressure, however recent research has shown that AmILs are toxic towards a variety of organisms such as microbes, plants, aquatic life and mammalian cells.⁶⁻¹⁰ While AmIL cytotoxicity is a potential environmental and human safety concern as these chemicals have been detected in soil samples,^{11, 12} their cytotoxicity towards cancer cells has triggered interest in their uses as anticancer agents. For example, AmILs have been shown to reduce the viability of a range of cancer cell lines, including breast (MCF-7, MDA-MB-231), cervical (HeLa), leukemia (IPC-81) and colon cancer (HT-29 and CaCo-2).^{9, 13-16}

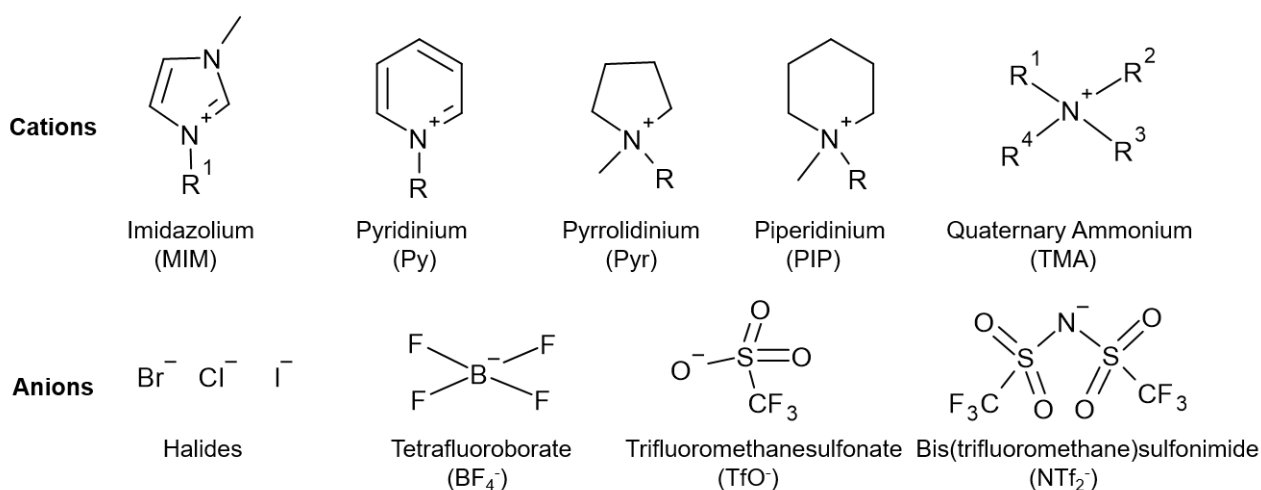


Figure 1 Chemical structures of common AmIL cationic headgroups (upper) and anions (lower). The cationic headgroups of AmILs are substituted with an alkyl chain.

The cytotoxicity of AmILs is dependent on their chemical structure and some structure-activity relationships (SARs) have emerged. AmILs possess a cationic headgroup substituted with an alkyl chain and many studies have shown that increased alkyl chain length is a major determinant of AmIL cytotoxicity.^{7, 9, 13, 16-22} AmILs with aromatic cationic headgroups (eg imidazolium, pyridinium) are generally more cytotoxic than AmILs with structurally related but aliphatic cationic headgroups, although this effect is observed only for AmILs with longer (\geq C8) alkyl chains.¹⁵ For example [C₈Py][Br], an AmIL with an octyl-substituted pyridinium headgroup, decreased the viability of MCF-7 breast cancer cells with 25-fold greater potency than its piperidinium-based counterpart, while [C₃Mim][NTf₂] was equipotent to its pyrrolidinium counterpart.¹⁵ The effect of the anion on AmIL cytotoxicity is less clear, with some studies showing that the anion affects cytotoxicity,^{7, 23} whilst others have shown there to be no effect.^{10, 13, 19, 21} In general it appears that the bis(trifluoromethane)sulfonimide (NTf₂) anion has the greatest impact on AmIL toxicity, although the NTf₂ anion is cytotoxic in its own right (MTT IC₅₀ of LiNTf₂ in HeLa cells = 4.24 μ M).^{10, 24} There is some evidence that the influence of the anion on AmIL cytotoxicity is dependent on the nature of the cation, and that the anion does not affect the cytotoxicity of AmILs with longer alkyl chains or aromatic cationic headgroups.¹⁵

The cellular mechanism/s by which AmILs exert cytotoxicity has not been fully elucidated, however a growing body of evidence suggests that AmILs kill cells by either disrupting cellular membranes or inducing mitochondrial dysfunction.⁶ Numerous studies have shown that AmILs effectively partition into model lipid bilayers and disrupt membrane integrity,^{25, 26} and cell-based studies suggest that permeabilisation of the plasma may account for their cytotoxic effects.^{24, 25, 27-31} A correlation between AmIL lipophilicity and their ability to disrupt cell membranes have been shown in several studies, where increasing chain length leads to greater membrane disruption and cytotoxicity.^{9, 13, 16, 19, 32} Increased cytotoxicity has been attributed to the greater lipophilicity of long chain AmILs, which promotes their partitioning into lipid bilayers.^{10, 13, 33} Similarly, improved

lipophilicity and membrane penetration of aromatic AmILs relative to aliphatic AmILs could account for their greater cytotoxicity.³⁴ Apart from membrane disruption, AmILs have been shown to cause mitochondrial dysfunction in human cell lines.^{20,30} Mitochondria contain a permeable outer membrane and an impermeable inner mitochondrial membrane (IMM) that encloses the mitochondrial matrix. In respiring mitochondria the electron transport chain pumps protons across the IMM, and the resulting proton gradient polarises the IMM and establishes the mitochondrial membrane potential ($\Delta\Psi_M$). Several studies have shown that AmILs can collapse the $\Delta\Psi_M$.³⁵⁻³⁷ Alteration of $\Delta\Psi_M$ is significant because mitochondria utilise $\Delta\Psi_M$ for the production of ATP via oxidative phosphorylation.³⁸ For example, [C₈mim][Cl] has been shown to reduce intracellular ATP levels, which leads to cell death.³⁰ AmILs -induced alterations in mitochondrial function have also been linked to an overproduction of reactive oxygen species (ROS), which can damage DNA, enzymes and membrane lipids.^{6,20} There are also reports of AmILs causing a release of mitochondrial calcium into the cytoplasm, cytochrome C release, altered cell signalling pathways, and DNA fragmentation.^{10,20,24,30,35,37,39-42} The precise cellular targets that AmILs interact with to produce these effects has not been established.

AmILs, particularly those with aromatic cationic headgroups and delocalised positive charge, share physicochemical properties with lipophilic cations such as triphenylphosphoniums (TPP). Lipophilic cations are widely used in mitochondrial research because they readily pass through cellular membranes and are extensively taken up by the mitochondria due to electrostatic interactions with the mitochondrial $\Delta\Psi_M$.⁴³⁻⁴⁵ Lipophilic cations are therefore used to stain mitochondria for microscopy (eg MitoTracker dyes) and to selectively deliver drugs and other cargo to the mitochondria.⁴⁴ For example, the therapeutically approved antioxidant MitoQ consists of a TPP cation linked via a decyl chain to an antioxidant ubiquinol moiety.⁴⁶ When delivered *in vitro* or *in vivo*, MitoQ accumulates in mitochondria and localises in the IMM, where the ubiquinol moiety embeds in the hydrophobic core of the IMM and protects it from lipid peroxidation.

Given that some AmILs possess lipophilic cations, and in particular AmILs with aromatic headgroups substituted with longer alkyl chains, we hypothesised that these AmILs would accumulate in mitochondria and partition into the IMM. Furthermore, given the well-established capacity for AmILs to disrupt membrane integrity, we anticipated that AmILs would permeabilise the IMM and produce a series of effects that contribute to cell death. To test this we studied the subcellular localisation of a fluorescent AmIL by confocal fluorescence microscopy. Next, the cytotoxic IC₅₀ concentrations of a series of AmILs containing aromatic or aliphatic cations substituted with butyl or decyl alkyl chains was determined, and the effects of these AmILs on mitochondrial function at their IC₅₀ concentrations was assessed. In contrast to short chain and/or aliphatic AmILs, those with aromatic long chain cations produced cellular effects consistent with permeabilisation of the IMM, including depolarisation of the IMM, inhibition of oxidative phosphorylation and ATP production, and an increase in intracellular ROS. Combined, these data provide evidence that AmILs with aromatic long chain cations target the IMM to induce cell death.

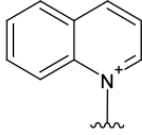
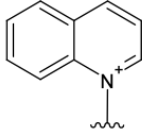
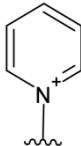
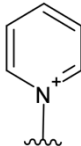
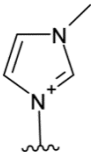
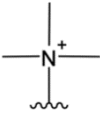
Results and discussion

AmIL library design and effects on cell viability

For this study a library of AmILs were prepared to investigate the impact of different cations on cytotoxicity and mitochondrial actions (Table 1). ILs substituted with butyl (C₄-AmILs) or decyl (C₁₀-AmILs) alkyl chains on the cationic headgroups were included as alkyl chain length has a strong influence on AmIL cytotoxicity^{7,9,13} and their capacity to permeabilise lipid bilayers.^{25,26} AmILs with aromatic (methylimidazolium, pyridinium and quinolinium) and aliphatic (trimethylammonium) headgroups were included to investigate the effect of aromaticity on activity. It was anticipated that delocalisation of cationic charge across the aromatic headgroup would increase the lipophilicity of aromatic AmILs and therefore promote mitochondrial uptake. AmILs were either purchased from commercial suppliers or synthesised in a single step by neat reactions of the heterocycle with the corresponding alkyl bromide (see SI for details).

We first assessed the cytotoxicity of the AmILs against HeLa cervical cancer cells and BEAS-2B lung epithelial cells using the MTS assay. In the MTS assays, and all other assays, the final concentration of DMSO in the assay media was $\leq 0.1\%$ as DMSO can affect the permeability of cell membranes at concentrations exceeding 2%,⁴⁷⁻⁴⁹ and 0.1% DMSO has been used in previous studies^{7,24} assessing AmIL cytotoxicity (see SI for full details of assay solutions). The AmILs produced dose-dependent reductions in cell viability and the dose-response curves (Figure S1) were used to calculate IC₅₀ concentrations (Table 1). The observed potencies of the AmILs bearing Mim- and Py- based head groups were similar to those reported for these AmILs,^{7,9,10,19,50} for example in our study [C₄Mim][Br] reduced HeLa cell viability at an IC₅₀ concentration of 13.88 ± 1.84 mM which is comparable to a previously reported IC₅₀ value of 2.75 ± 0.69 mM.¹⁰ The IC₅₀ concentrations of the aromatic C₁₀AmILs in both cell lines (27-110 μ M) were comparable to known cytotoxins such as the herbicide paraquat (IC₅₀ = 72.3 μ M against HeLa cells)⁵¹ and the anticancer agents doxorubicin (IC₅₀ = 2.4 μ M against HeLa cells)⁵², which suggests that the longer chain AmILs are potent cytotoxic agents.

Table 1 Cytotoxicity of AmILs against HeLa and BEAS-2B cell lines. IC₅₀ concentrations were determined using MTS assays after 48-hour treatments.

AmIL	Headgroup structure	HeLa IC ₅₀ (mM)	BEAS-2B IC ₅₀ (mM)
[C ₄ Quin][Br]		2.24 ± 0.06	1.64 ± 0.22
[C ₁₀ Quin][Br]		0.0268 ± 0.0003	0.03284 ± 0.00346
[C ₄ Py][Br]		13.31 ± 1.18	15.70 ± 1.40
[C ₁₀ Py][Br]		0.0888 ± 0.0003	0.10261 ± 0.00502
[C ₄ Mim][Br]		13.88 ± 1.84	16.98 ± 0.86
[C ₄ Mim][BF ₄]		11.80 ± 0.36	18.37 ± 1.42
[C ₄ Mim][CF ₃ SO ₃]		10.47 ± 0.28	14.05 ± 0.68
[C ₁₀ Mim][Br]		0.0848 ± 0.0006	0.11230 ± 0.00675
[C ₁₀ Mim][BF ₄]		0.0875 ± 0.0097	0.0909 ± 0.00143
[C ₁₀ Mim][CF ₃ SO ₃]		0.0849 ± 0.0021	0.0894 ± 0.00121
[C ₄ TMA][Br]		11.43 ± 1.23	39.93 ± 0.99
[C ₁₀ TMA][Br]		0.197 ± 0.0073	0.20197 ± 0.00903

The general trends in AmILs cytotoxicity are consistent with previous reports which found that alkyl chain length was a major determinant of activity.^{9, 19, 21, 53, 54} As shown in Table 1, short chain C₄-AmILs ILs had IC₅₀ concentrations in the millimolar range while those with longer decyl chains were in the micromolar range, regardless of headgroup structure or cell line. Headgroup aromaticity appeared to be an important factor determining cytotoxicity within the decyl-substituted series. Thus, [C₁₀TMA][Br] reduced the viability of both HeLa and BEAS-2B cells with IC₅₀ concentrations of ~200 μM, while the aromatic AmILs [C₁₀Mim][Br] and [C₁₀Py][Br] were 2 fold more potent (IC₅₀ concentrations of ~100 μM, P < 0.05). The quinolonium-based AmILs [C₁₀Quin][Br] was the most potent in the series and reduced the viability of both cells lines IC₅₀ concentrations of ~30 μM, which

suggests that larger cationic headgroups promote cytotoxicity. Interestingly, the nature of the cationic headgroup did not have a significant impact on the cytotoxicity of the short chain C₄-AmILs [C₄Mim][Br], [C₄Py][Br] and [C₄TMA][Br], with these AmILs reducing the viability of HeLa cells with IC₅₀ concentrations of ~12 mM, although [C₄Quin][Br] was $2.24 \pm 0.06 \mu\text{M}$. In general the IC₅₀ concentrations were higher in BEAS-2B cells relative to HeLa cells, suggesting that the cancer cell line was more susceptible to AmILs cytotoxicity.

To determine whether the anion has an influence on cytotoxicity, the anionic component of [C₄Mim][Br] and [C₁₀Mim][Br] was exchanged with trifluoromethanesulfonate (CF₃SO₃⁻) and tetrafluoroborate (BF₄⁻) anions. The IC₅₀ concentrations for the [C₄Mim] and [C₁₀Mim] AmILs were similar in both cell lines, regardless of the anion ($P > 0.05$), despite differences in the ionic strength and lipophilicity of the anions (Table 1), showing that the cytotoxicity of these compounds is unaffected by the nature of the anion. This is supported by several studies which show that the cytotoxicity of imidazolium AmILs are not affected by the anionic component.^{13, 55-58}

AmILs cytotoxicity is associated with their ability to permeabilise lipid bilayers

As cell membranes are a suspected target of cytotoxic AmILs^{19, 22, 28, 59} we assessed the capacity of the AmILs to disrupt membrane integrity using tethered bilayer lipid membranes (tBLMs). This system is comprised of a lipid bilayer tethered to a thin film gold electrode, and permeabilisation of the lipid bilayer is detected as an increase in ionic membrane conductance, as measured by electrical impedance spectroscopy.⁶⁰ For this study tBLMs were assembled with 1,2-dioleoyl-sn-glycero-3-phosphocholine (DOPC), which is the major phospholipid component of the IMM,⁶¹ and treated with each AmIL at a common concentration of 200 μM (Figure 2) and at their MTS IC₅₀ concentrations (Figure S5).

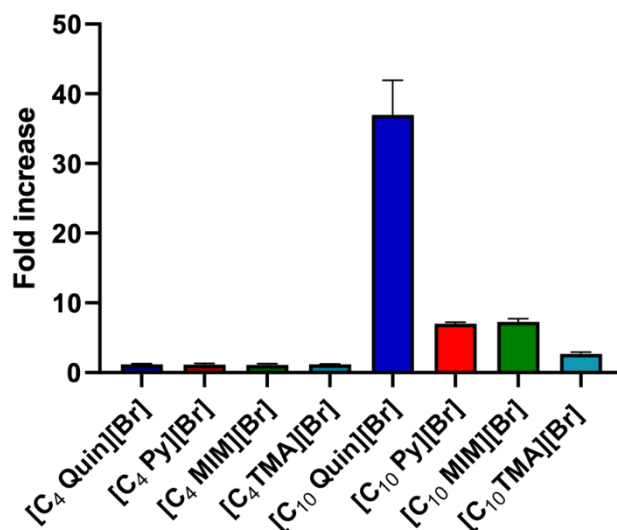


Figure 2 Effects of AmILs (200 μ M) on the conductance of DOPC lipid bilayers tethered to gold electrodes, as measured by electrical impedance spectroscopy. Data normalised to membrane conductance prior to AmIL treatment at pH = 7. Data represents the mean of 2 independent experiments.

As shown in Figure 2, addition of C₁₀-AmILs significantly increased bilayer conductance. [C₁₀Mim][Br] and [C₁₀Py][Br] increased conductance 7-fold, whilst [C₁₀Quin][Br] produced a 33-fold increase. The aliphatic [C₁₀TMA][Br] had the smallest effect of the C₁₀-AmILs, with tBLM conductance increasing 2.5 fold. In contrast the short chain C₄-AmILs did not have a statically significant effect on bilayer conductance. The observed activities are consistent with previous studies which have shown larger alkyl tails and cationic headgroup size promote AmIL induced membrane disruption.^{25, 27}

Importantly, the trends in membrane effects reflect with the cell viability IC₅₀ data (Table 1). Thus, the C₄-AmILs failed to increase membrane conductance, and these AmILs killed HeLa and BEAS-2B cells with relatively high IC₅₀ concentrations in the millimolar range. In contrast, the C₁₀-AmILs increased tBLM membrane conductance and had MTS IC₅₀ concentrations in the micromolar range. Furthermore, the MTS IC₅₀ concentrations and membrane conductance increased produce by

the C₁₀-AmILs correlated (Figure S3). This correlation suggests that the cytotoxicity of the C₁₀-AmILs is associated with the capacity to disrupt cellular membranes.

Quinilium-based AmIL accumulate in HeLa cell mitochondria

The next question that arises is which cellular membrane is targeted by C₁₀-AmILs to induce cell death. We anticipated that C₁₀-AmILs would target the IMM as other lipophilic cations such as MitoQ are known to accumulate at this membrane, and mitochondria are sites of critical cellular process, as well as regulators of cell death. To provide some insight we studied the subcellular localisation of AmILs by taking advantage of the fact that quinilium-based AmILs are fluorescent and can be tracked by confocal microscopy. Thus, cellular imaging and colocalisation experiments were carried out using HeLa cells treated with Mitotracker deep red ($\lambda_{\text{ex}}/\lambda_{\text{em}}$ 644/665 nm), Hoechst ($\lambda_{\text{ex}}/\lambda_{\text{em}}$ 350/461 nm) and [C₄MeQuin][I] ($\lambda_{\text{ex}} = 488$ nm), a methyl-substituted analogue of [C₄Quin][Br] with optical properties suitable for confocal microscopy (see SI for details). A butyl chain was incorporated into [C₄MeQuin][I] to minimise its ability to depolarise HeLa mitochondria and interfere with Mitotracker deep red staining.

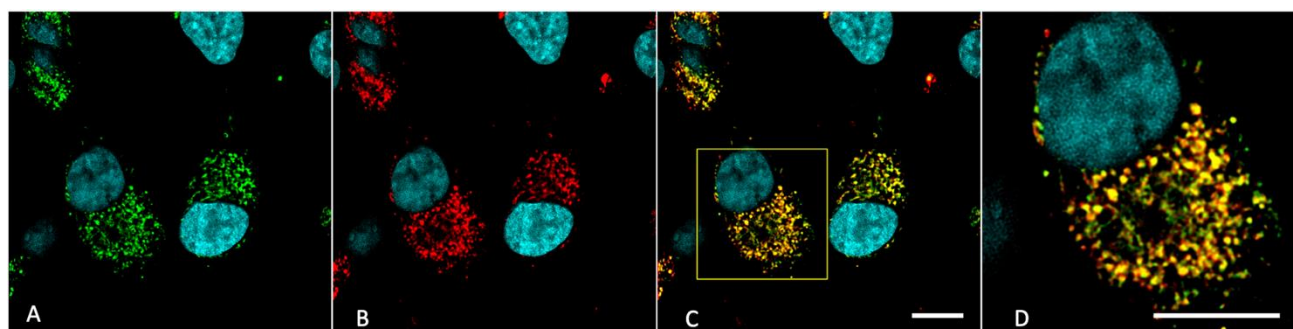


Figure 3 Confocal fluorescence microscopy of $[C_4MeQuin][I]$ in HeLa cells reveals mitochondrial specificity. A maximum intensity projection of the labelled cell volume. (A) Green channel $[C_4MeQuin][I]$ (500nM, $\lambda_{ex}= 488$ nm). (B) Red channel Mitotracker Deep Red (200 nM, $\lambda_{ex}= 644$ nm). (C) Merged channels. (D) Magnified view of boxed region in (C). Blue channel in all cases: Hoechst nuclear stain (4 μ M, $\lambda_{ex}/\lambda_{em}$ 350/461 nm) Scale Bar (10 μ m).

Confocal microscopy (Figure 3) revealed that $[C_4MeQuin][I]$ exhibited high levels of colocalisation with Mitotracker Deep Red 20 minutes after addition to HeLa cells. This is clearly evident with the green fluorescence of $[C_4MeQuin][I]$ in the green channel overlapping with the red fluorescence of Mitotracker Deep Red (Figure 3C). Single colour controls (data not shown) confirmed the channel specificity of $[C_4MeQuin][I]$ and Mitotracker Deep Red to the green and red channels respectively and no bleed through was observed between channels. A colocalization analysis of the green and red channels revealed a Pearson's correlation (PC) coefficient: 0.94, further confirming the localisation of $[C_4MeQuin][I]$ within the mitochondria of HeLa cells. Significant accumulation of $[C_4MeQuin][I]$ in the nucleus was not observed, as shown by the lack of colocalisation of $[C_4MeQuin][I]$ with the Hoechst nuclear stain (blue channel in Figure 3, and Figure S6). This study therefore indicates that like other lipophilic cations, $[C_4MeQuin][I]$ accumulates in the mitochondria of HeLa cells in response to the mitochondrial membrane potential.

Effects of AmILs on mitochondrial function in HeLa cells

The fluorescent microscopy images and association between the MTS IC_{50} and tBLM data suggest that the C_{10} -AmILs in this study exert their cytotoxic actions at the IMM. That the IMM is the target of C_{10} -AmILs is reasonable given that mitochondria play critical roles in cell function and death, and the integrity of the IMM influences these functions.⁶² The primary role of mitochondria is to convert nutrients to ATP through oxidative phosphorylation (OxPhos). During OxPhos a series of IMM-embedded proteins called the electron transport chain (ETC) use energy derived from nutrient oxidation to pump protons across the IMM. As the IMM is relatively impermeable, a proton gradient across the IMM is established that generates the mitochondrial membrane potential ($\Delta\psi_M$), and $\Delta\psi_M$ is used to catalyse ATP production by ATP-synthase. Drugs that disrupt OxPhos and ATP production (mitochondrial uncouplers) can induce cell death and are currently being explored as anticancer agents,⁶³ and several studies have suggested that imidazolium-based AmILs affect OxPhos.^{20, 30, 64} Mitochondria are also sites of reactive oxygen species (ROS) production and regulate intracellular calcium levels, both of which are important to cell health, and release pro-apoptotic proteins to carry out programmed cell death. It follows that drugs that induce mitochondrial dysfunction can produce cytotoxicity.

A series of experiments were therefore undertaken to understand how the AmILs in this study affected mitochondrial function in HeLa cells. For these studies HeLa cells were treated with the AmILs at their MTS IC_{50} concentrations (Table 1) for short time periods to capture the early cellular effects that occur during cell death. Initially Seahorse Mito Stress tests were performed on HeLa cells pre-treated with the AmILs (Figure 4) to detect changes in mitochondrial function and OxPhos. It should be noted that while cancer cells do show a shift towards ATP production via glycolysis (the Warberg effect), OxPhos still appears to be an important source of ATP production in cancer cells.⁶⁵⁻

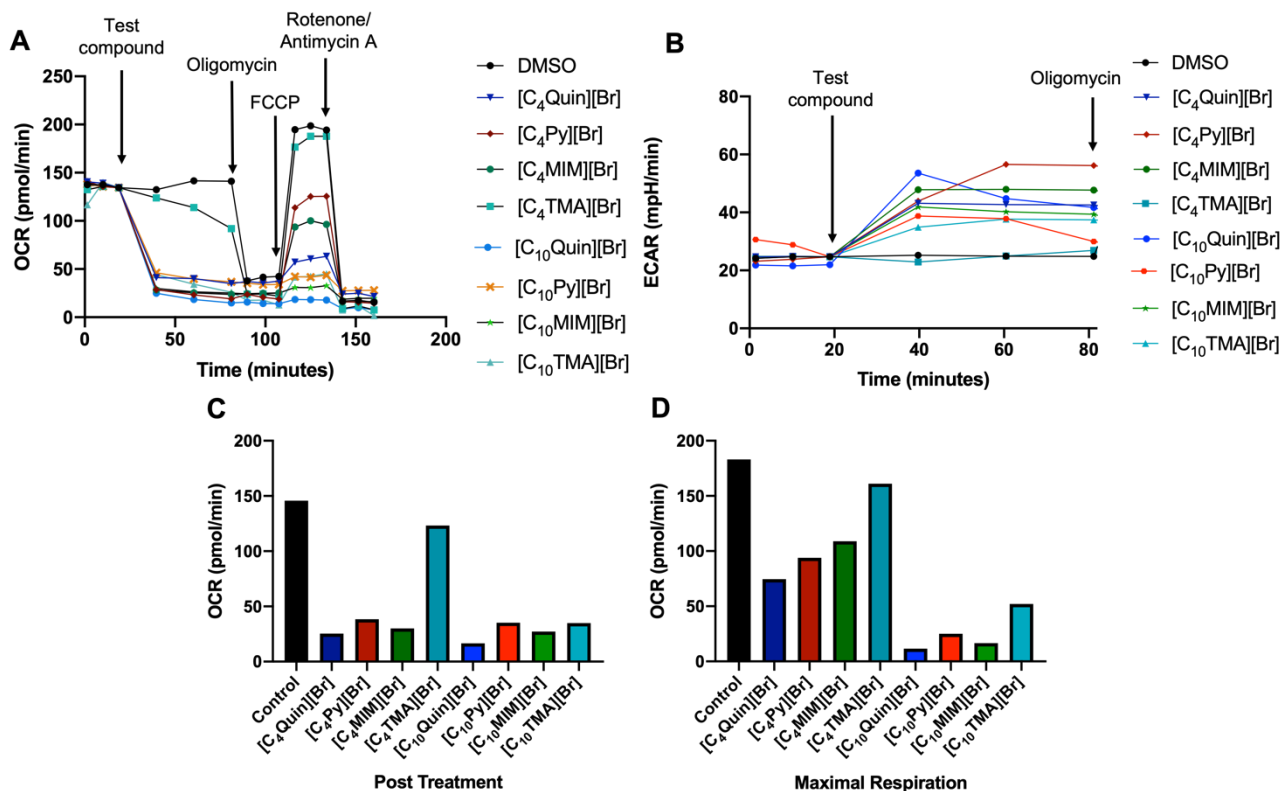


Figure 4 (A) The effect of AmILs on oxygen consumption rate (OCR) in HeLa cells. The sequential addition of the AmILs the MTS IC₅₀ concentrations, oligomycin a mitochondrial ATP-synthase inhibitor (1 μM), the protonophore FCCP (2 μM) and the electron transport chain complex inhibitors rotenone/antimycin A (1 μM). (B) ECAR of HeLa cells following the treatment of ILs. (C) Determination of OCR associated with post treatment in HeLa cells following the treatment of ILs. (D) Determination of OCR associated with maximal respiration in HeLa cells following the treatment of ILs. DMSO was used as a negative control with a final concentration of 0.1% in the well. Data represents the average value of 2 wells from the same experiment.

As shown in Figure 4 (panels A and C), all AmILs except [C₄TMA][Br] produced a rapid decrease in cellular oxygen consumption rate (OCR) HeLa cells, which is proportional to OxPhos, and an associated increase in extracellular acidification rate (ECAR, Figure 4B), which is proportional to glycolysis. These data suggest that these AmILs inhibit OxPhos, and in response the cells shift from

OxPhos to glycolysis to generate ATP,¹¹ and are consistent with previous data showing that methylimidazolium-based AmILs decrease OCR and increased in ECAR in B-13 hepatocytes.⁶⁸

Maximal respiration, which is measured after the addition of FCCP, reflects the functional capacity of the ETC. With the exception of [C₄TMA][Br], all AmILs reduce maximal respiration compared to control (Figure 4D), which is a strong indicator that these AmILs induce mitochondrial dysfunction.^{69, 70} In cells treated with aromatic C₁₀-AmILs [C₁₀Quin][Br], [C₁₀Mim][Br] and [C₁₀Py][Br], but not [C₁₀TMA][Br] and the C₄-AmILs, maximal respiratory capacities were below post-treatment levels, indicating these cells did not have any spare respiratory capacity. This is significant as spare respiratory capacity is another indicator of the mitochondria's ability to respond to increased respiratory requirement during cell stress, where low capacities indicate an inability of the mitochondria to provide the increased need for ATP during stress.^{24, 70, 71} Combined, the seahorse data shows that AmILs affect OxPhos at their MTS IC₅₀ concentrations, and that only the C₁₀-AmILs reduce spare respiratory capacity and ability to respond to stress.

The integrity of the IMM is critical to maintaining the mitochondrial membrane potential and ATP synthesis via OxPhos. Given the results from the fluorescence microscopy and tBLM studies, it was suspected that inhibition of OxPhos may result from AmILs-mediated permeabilisation of the IMM and collapse of the proton gradient across this membrane. To assess this we measured the ability of AmILs to depolarise the IMM in HeLa cell mitochondria using the JC-1 assay. JC-1 is a redox active lipophilic cationic dye that forms aggregates that fluoresce red in the electronegative environment of polarised mitochondria. In response to depolarisation of the IMM, JC-1 leaves mitochondria and disaggregates to monomers that fluoresces green. Thus changes in JC-1 red:green fluorescence ratio can be used to detect changes in IMM depolarisation.

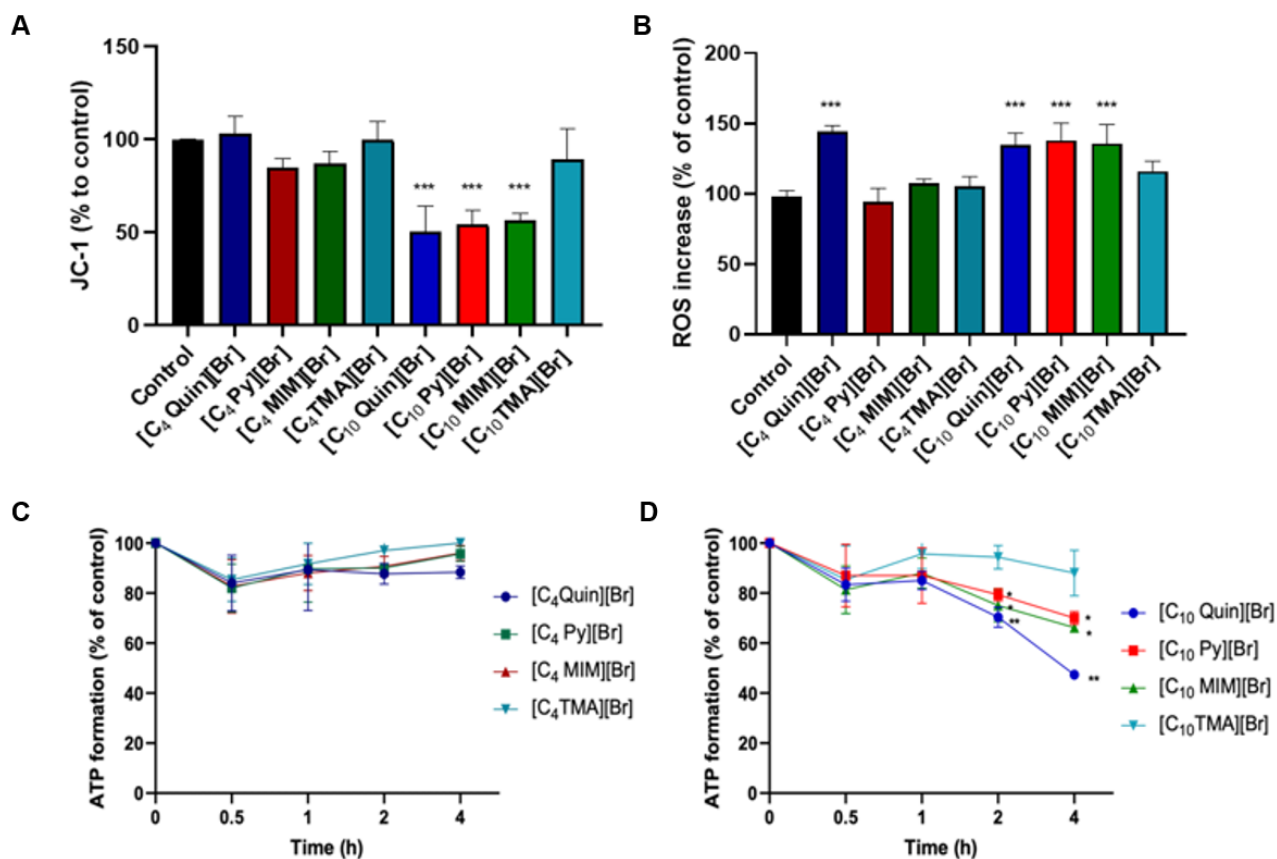


Figure 5 Effects of AmILs on mitochondrial function in HeLa cells. (A) JC-1 red:green fluorescence ratio as percentage of DMSO-treated control in HeLa cells treated for 1 hr at the MTS IC₅₀ concentration. (B) Total intracellular ROS production in HeLa cells treatment with AmILs at their IC₅₀ concentrations (6 h). (C) and (D) Total intracellular ATP levels in HeLa cells following treatment with either the C₄-AmILs (panel C) or C₁₀-AmILs (panel D) at their MTS IC₅₀ concentrations. ATP levels are expressed as percentage of time-matched DMSO control. All data represents the mean ± SEM of 3 independent experiments. Different from DMSO-treated control: (*) P < 0.05, (**) P < 0.01 (***), P < 0.001.

As shown in Figure 5A aromatic C₁₀-AmILs [C₁₀Quin][Br], [C₁₀Mim][Br] and [C₁₀Py][Br] caused a shift in the JC-1 red:green fluorescence ratio to 50-56% of control after 1 hour treatments, which indicates that these AmILs rapidly collapse the IMM proton gradient. In contrast, the aliphatic

C₁₀-AmILs [C₁₀TMA][Br] and all C₄-AmILs (Figure 5A) had no activity in JC-1 assays, which suggests that these AmILs do not affect the IMM polarisation.

We next measured intracellular ATP levels in HeLa cells treated with the AmILs at their MTS IC₅₀ concentrations. ATP levels were monitored over 4 hours because no loss in cell viability was observed over these short treatment periods (see Table S1). As shown in Figure 5D aromatic C₁₀-AmILs [C₁₀Quin][Br], [C₁₀Mim][Br] and [C₁₀Py][Br] decreased intracellular ATP levels. [C₁₀Quin][Br] had the greatest effect, reducing intracellular ATP to 47 ± 0.72 % of control after 4 hours, while [C₁₀Mim][Br] and [C₁₀Py][Br] produce a similar decreases of ~68 %. In contrast, the aliphatic C₁₀-AmILs [C₁₀TMA][Br] and all C₄-AmILs (Figure 5C) did not significantly decrease ATP production. Considered together with the JC-1 data, it can be concluded that of the AmILs studied, only the aromatic C₁₀-AmILs can permeabilise and depolarise the IMM at their MTS IC₅₀ concentrations to such an extent that is detected in the JC-1 assays and leads to impaired ATP production. This aligns with the Seahorse analysis which showed that HeLa cells treated with aromatic C₁₀-AmILs lacked spare respiratory capacity, and the tBLM data which showed these AmILs have the largest effect in membrane conductance. Considering that in the mitochondrial assays [C₁₀Quin][Br], [C₁₀Mim][Br] and [C₁₀Py][Br] were tested at 25-90 μ M, while [C₁₀TMA][Br] (200 μ M) and C₄-AmILs (2-15 mM) were tested at much higher concentrations, it is clear that the aromatic C₁₀-AmILs have a much greater capacity to affect mitochondrial respiration. The relatively lipophilic nature of the aromatic C₁₀-AmILs, which results from their larger alkyl chains and delocalised positive charge, likely accounts for the capacity of these AmILs to accumulate in, and permeabilise, the IMM.

Finally, the capacity of the AmILs to induce ROS formation was assessed. Mitochondria are major sources of ROS and several studies have shown that aromatic AmILs cause an overproduction of ROS that leads to cell death, although the precise mechanism for ROS production is unknown.^{10,30,68,72-75} Recently Wright *et al* proposed that Mim-based AmILs can be reduced by the electron transport chain (ETC) to neutral radical species that undergo redox cycling to produce ROS.⁶⁸ Efficient ROS

production was only induced by Mim-based AmILs with long chains ($\geq C_6$), which the authors hypothesised was due to partitioning of these more lipophilic AmILs in the IMM where the ETC is located. Alternatively, the pore forming agent alamethicin has been shown to induce ROS formation in isolated mitochondria by permeabilising the IMM, and it is possible that the AmILs in this study could increase ROS by this mechanism.⁷⁶

ROS production in HeLa cells treated with the AmILs at their MTS IC₅₀ concentrations was assessed using the DCFDA assay (Figure 5B). Consistent with previous findings,⁶⁸ the imidazolium based [C₁₀Mim][Br] increased intracellular ROS levels to ~140% of control. The remaining aromatic C₁₀-AmILs [C₁₀Quin][Br] and [C₁₀Py][Br] also produced similar increases in ROS. In contrast, the aliphatic C₁₀-AmILs [C₁₀TMA][Br] and C₄-ILs [C₄TMA][Br], [C₄Mim][Br] and [C₄Py][Br] did not induce ROS formation. The inactivity of these more polar AmILs may result from their decreased capacity to accumulate in and depolarise the IMM, or in the case of the aliphatic AmILs, an inability to efficiently produce ROS through the redox cycling mechanism proposed by Wright *et al.* Interestingly [C₄Quin][Br] increased ROS to similar levels as the aromatic C₁₀-AmILs. This is likely due to the larger quinolinium headgroup which renders [C₄Quin][Br] sufficiently lipophilic to accumulate in the IMM.

Taken together, the data presented shows that AmILs containing aromatic cationic headgroups substituted with decyl alkyl tails target the IMM in HeLa cells and induce mitochondrial dysfunction at concentrations relevant to their cytotoxicity. Subsequent permeabilisation and depolarisation of the IMM inhibits ATP synthesis by OxPhos and also leads to overproduction of ROS. These effects occur in HeLa cells treated with the aromatic C₁₀-AmILs at their MTS IC₅₀ concentrations over short time periods, which suggests these effects may be early cellular events that result in cell death. In support of this, increased ROS is a known trigger of cell death, and dissipation of the proton gradient across the IMM and uncoupling of OxPhos by protonophores can induce cell death. Indeed, the use of mitochondrial uncouplers as clinical anticancer agents is currently being explored.⁶³ Given that

numerous studies have suggested that AmILs exert their cytotoxic actions by targeting either cell membranes or inducing mitochondrial dysfunction, our findings provide an important insight that it specifically is the IMM that is targeted by long chain aromatic AmILs due to the lipophilic nature of their cations.

Short chain (C_4) and aliphatic AmILs also appear to affect mitochondrial function in Seahorse assays, albeit at much higher concentrations and to lesser extents than the aromatic C_{10} -AmILs, however measurable effects on $\Delta\Psi_M$ in JC-1 assays, ATP production and ROS levels were not seen (with the exception of [C₄Quin][Br]). These data therefore suggest that short chain and/or aliphatic AmILs kill cells through a different mechanism, which also corresponds to a drop in cytotoxicity (IC_{50} concentrations in the millimolar range, compared to micromolar range for aromatic long chain AmILs). The reduced activity of the aliphatic and short chain AmILs likely results from the inability of these AmILs to efficiently accumulate into and permeabilise the IMM. An exception is [C₄Quin][Br], which increased ROS but did not effect JC-1 red:green ratios or ATP levels in HeLa cells. One possible explanation is that due to its larger headgroup [C₄Quin][Br] is sufficiently lipophilic to accumulate in the IMM where it produces ROS through redox cycling but lacks a sufficiently long alkyl chain to permeabilise and depolarise the IMM, and inhibit ATP production.

The mechanism proposed in this paper can be used to explain some aspects of the SAR governing AmIL cytotoxicity, as structural features that increase the capacity of AmILs to disrupt mitochondrial function should also be expected to promote cytotoxicity. To target the IMM and induce cell death, AmILs must be sufficiently lipophilic to diffuse through the plasma membrane, and an alkyl chain long enough to disrupt the integrity of the IMM. Consistent with this, SAR studies have shown that increased alkyl chain length is a major determinant of AmIL cytotoxicity.^{7, 9, 13, 16-22} Aromatic AmILs are in general more cytotoxic than their aliphatic counterparts,¹⁵ which can be explained by delocalisation of the cationic charge that renders aromatic AmILs more lipophilic than aliphatic AmILs. Headgroup aromaticity has less impact on the cytotoxicity of short chain AmILs, which may

result because these AmILs kill cells by a different mechanism. Finally, there are conflicting reports regarding the influence of the anion, although it appears the nature of the anion has the least impact on the cytotoxicity of aromatic AmILs with long alkyl chains.¹⁵ This too can be rationalised by the proposed mechanism as it is only the cation that plays a role in the mitochondrial effects.

Conclusions

AmILs share physiochemical properties with lipophilic cations and were therefore anticipated to target the IMM to induce cell death. Using fluorescence microscopy we showed that a quinolinium-based AmIL is rapidly taken up into HeLa cells mitochondria. The capacity of a series of AmILs to reduce viability and induce mitochondrial dysfunction in HeLa cells was assessed. AmILs bearing aromatic headgroups substituted with decyl chains were the most effective at inducing cell death and permeabilising lipid bilayers. When tested at the MTS IC₅₀ concentrations, long chain aromatic AmILs produced a variety of cellular effects consistent with permeabilisation of the IMM. These effects are associated with cell death, and therefore indicate long chain aromatic AmILs kill cells by targeting the IMM. AmILs with short chains or aliphatic headgroups failed to produce these effects which suggested these AmILs produce cytotoxicity by an alternate mechanism. These findings provide new mechanistic insights into AmIL cytotoxicity and may assist in the design of task specific AmILs for safe industrial application or as anticancer agents.

Author Contributions

- M. Duman performed the synthesis, isolation, biological assays, data analysis, and wrote the manuscript
- A. Angeloski performed optical measurements and revised the manuscript
- M.S. Johnson performed optical microscopy and image analysis
- T. Rawling provided conceptual advice and revised the manuscript

Conflicts of interest

There are no conflicts to declare.

References

1. T. Welton, *Chem. Rev.*, 1999, **99**, 2071-2084.
2. D. Zhao, M. Wu, Y. Kou and E. Min, *Catal. Today.*, 2002, **74**, 157-189.
3. A. A. C. Toledo Hijo, G. J. Maximo, M. C. Costa, E. A. C. Batista and A. J. A. Meirelles, *ACS Sustain. Chem. Eng.*, 2016, **4**, 5347-5369.
4. H. Qi, Y. Ren, S. Guo, Y. Wang, S. Li, Y. Hu and F. Yan, *ACS Applied Materials & Interfaces.*, 2020, **12**, 591-600.
5. V. Kumar and S. V. Malhotra, *Bioorg Med Chem Lett.*, 2008, **18**, 5640-5642.
6. P. Kumari, V. V. S. Pillai and A. Benedetto, *Biophys. Rev.*, 2020, **119**, 274-286.
7. M. Cvjetko, K. Radošević, A. Tomica, I. Slivac, J. Vorkapić-Furač and V. G. Srček, *Arh Hig Rada Toksikol.*, 2012, **63**, 15-20.
8. N. K. Kaushik, P. Attri, N. Kaushik and E. H. Choi, *Molecules.*, 2012, 13727-13739.
9. P. Stepnowski, A. C. Składanowski, A. Ludwiczak and E. Laczyńska, *Hum. Exp. Toxicol.*, 2004, **23**, 513-517.
10. X. Wang, C. A. Ohlin, Q. Lu, Z. Fei, J. Hub and P. J. Dysonc, *Green. Chem.*, 2007, 1191-1197.
11. P. M. Probert, A. C. Leitch, M. P. Dunn, D. E. Jones, P. G. Blain and M. C. Wright, *J. Hepatol.*, 2018, **69**, 1123-1135.
12. A. C. Leitch, T. M. Abdelghany, P. M. Probert, M. P. Dunn, S. K. Meyer, J. M. Palmer, M. P. Cooke, L. I. Blake, K. Morse, A. K. Rosenmai, A. Oskarsson, L. Bates, R. S. Figueiredo, I. Ibrahim, C. Wilson, N. F. Abdelkader, D. E. Jones, P. G. Blain and M. C. Wright, *Food Chem. Toxicol.*, 2020, **136**, 111069.
13. J. Ranke, K. Mölter, F. Stock, U. Bottin-Weber, J. Poczobutt, J. Hoffmann, B. Ondruschka, J. Filsera and B. Jastorffa, *Ecotoxicol. Environ. Saf.*, 2004, **58**, 396-404.

14. J. Salminen, N. Papaiconomou, R. A. Kumara, J.-M. Lee, J. Kerr, J. Newman and J. M. Prausnitz, *Fluid Ph. Equilibria.*, 2007, **261**, 421-426.
15. R. A. Kumar, N. Papaiconomou, J.-M. Lee, J. Salminen, D. S. Clark and J. M. Prausnitz, *Environ Toxicol.*, 2009, **24**, 388-395.
16. A. García-Lorenzo, E. Tojo, J. Tojo, M. Teijeira, F. J. Rodríguez-Berrocal, M. P. Gonzálezbd and V. S. Martínez-Zorzano, *Green Chem.*, 2008, **10**, 508-516.
17. R. F. M. Frade and C. A. M. Afonso, *Hum. Exp. Toxicol.*, 2010, **29**, 1038-1054.
18. M. C. Bubalo, K. Radošević, V. G. Srček, R. N. Das, PaulPopelier and KunalRoy, *Ecotoxicol. Environ. Saf.*, 2015, **112**, 22-28.
19. H. L. Chen, H. F. Kao, J. Y. Wang and G. T. Wei, *Chem. Soc.*, 2014, **61**, 763-769.
20. X.-Y. Li, C.-Q. Jing, W.-L. Lei, J. Li and J.-J. Wang, *Ecotoxicol. Environ. Saf.*, 2012, **83**, 102-107.
21. S. V. Malhotra and V. Kumar, *Bioorg. Med. Chem. Lett.*, 2010, **20**, 581-585.
22. I. Rusiecka and A. C. Składanowski, *Acta Biochim. Pol.*, 2011, **58**, 187-192.
23. V. Kumar and S. V. Malhotra, *Bioorg. Med. Chem. Lett.*, 2009, **19**, 4643-4646.
24. L. U. Dzhemileva, V. A. D'Yakonov, M. M. Seitkalieva, N. S. Kulikovskaya, K. S. Egorova and V. P. Ananikov, *Green. Chem.*, 2021, **23**, 6414-6430.
25. N. Kaur, M. Fischer, S. Kumar, G. K. Gahlay, H. A. Scheidt and V. S. Mithu, *J. Colloid Interface Sci.*, 2021, **581**, 954-963.
26. S. Kumar, H. A. Scheidt, N. Kaur, T. S. Kang, G. K. Gahlay, D. Huster and V. S. Mithu, *Langmuir*, 2019, **35**, 12215-12223.
27. N. Gal, D. Malferarri, S. Kolusheva, P. Galletti, E. Tagliavini and R. Jelinek, *Biochim. Biophys. Acta - Biomembr.*, 2012, **1818**, 2967-2974.
28. J. B, L. N, J. Qiu and Y. Zhu, *J. Phys. Chem. B.*, 2016, **120**, 2781-2789.

29. K. Cook, K. Tarnawsky, A. J. Swinton, D. D. Yang, A. S. Senetra, G. A. Caputo, B. R. Carone and T. D. Vaden, *Biomolecules*, 2019, **9**, 251.
30. X.-Y. Li, C.-Q. Jing, X.-Y. Zang, S. Yang and J.-J. Wang, *Toxicol In Vitro.*, 2012, **26**, 1087-1092.
31. S. Wu, L. Zeng, C. Wang, Y. Yang, W. Zhou, F. Li and Z. Tan, *J. Hazard. Mater.*, 2018, **348**, 1-9.
32. S. Stolte, J. Arning, U. Bottin-Weber, M. Matzke, F. S. K. Thiele, M. Uerdingen, U. Welz-Biermann, B. Jastorffa and J. Ranke, *Green Chem.*, 2006, **8**, 621-629.
33. R. Sheldon, *ChemComm.*, 2001, 2399-2407.
34. R. P. Austin, P. Barton, A. M. Davis, C. N. Manners and M. C. Stansfield, *J. Pharm. Sci.*, 1998, **87**, 599-607.
35. V. R. Thamke, A. U. Chaudhari, S. R. Tapase, D. Paul and K. M. Kodam, *Environ. Pollut.*, 2019, **250**, 567-577.
36. M. L. Stromyer, M. R. Southerland, U. Satyal, R. K. Sikder, D. J. Weader, J. A. Baughman, W. J. Youngs and P. H. Abbosh, *Eur. J. Med. Chem.*, 2020, **185**, 111832.
37. S. V. Malhotra, V. Kumar, C. Velez and B. Zayas, *MedChemComm.*, 2014, **5**, 1404-1409
38. L. D. Zorova, V. A. Popkov, E. Y. Plotnikov, D. N. Silachev, I. B. Pevzner, S. S. Jankauskas, V. A. Babenko, S. D. Zorov, A. V. Balakireva, M. Juhaszova, S. J. Sollott and D. B. Zorova, *Anal. Biochem.*, 2018, **552**, 50-59.
39. K. S. Egorova, E. G. Gordeev and V. P. Ananikov, *Chem. Rev.*, 2017, **117**, 7132-7189.
40. L. X, M. J and W. J, *Ecotoxicol. Environ. Saf.*, 2015, **120**, 342-348.
41. E. Gottlieb, S. M. Armour, M. H. Harris and C. B. Thompson, *Cell Death Differ.*, 2003, **10**, 709-717.
42. G. Kroemer, L. Galluzzi and C. Brenner, *Physiol. Rev.*, 2007, **87**, 99-163.

43. D. Guzman-Villanueva, M. R. Mendiola, H. X. Nguyen and V. Weissig, *SOJ pharm. pharm. sci.*, 2015, **2**, 1-9.
44. J. Zielonka, J. Joseph, A. Sikora, M. Hardy, O. Ouari, J. Vasquez-Vivar, G. Cheng, M. Lopez and B. Kalyanaraman, *Chem. Rev.*, 2017, **117**, 10043–10120.
45. M. T. Jeena, S. Kim, S. Jin and J.-H. Ryu, *Cancers.*, 2020, **12**.
46. S. T. Bond, J. Kim, A. C. Calkin and B. G. Drew, *Front Physiol.*, 2019, **10**, 543.
47. J. G. Gao, Y. Zhang, H. T. Zheng, C. F. Wang, H. X. Liu and S. C. Zhao, *Adv Mat Res.*, 2011, **236-238**, 2378-2382.
48. G. Da Violante, N. Zerrouk, I. Richard, G. Provot, J. C. Chaumeil and P. Arnaud, *Biol Pharm Bull.*, 2002, **25**, 1600-1603.
49. B. Gironi, Z. Kahveci, B. McGill, B.-D. Lechner, S. Pagliara, J. Metz, A. Morresi, F. Palombo, P. Sassi and P. G. Petrov, *Biophysical Journal*, 2020, **119**, 274-286.
50. S.A.Pérez, M.G.Montalbán, G.Carissimi, P.Licence and G.Víllora, *J. Hazard. Mater.*, 2020, **385**.
51. H. Shimada, K. Hirai, E. Simamura, T. Hatta, H. Iwakiri, K. Mizuki, T. Hatta, T. Sawasaki, S. Matsunaga, Y. Endo and S. Shimizu, *J Biol Chem.*, 2009, **284**, 28642-28649.
52. F. Benyettou, H. Fahs, R. Elkharrag, R. A. Bilbeisi, B. Asma, R. Rezugui, L. Motte, M. Magzoub, J. Brandel, J. C. Olsen, F. Piano, K. C. Gunsalus, C. Platas-Iglesias and A. Trabolsi, *RSC Adv.*, 2017, **7**, 23827-23834.
53. M. C. Bubalo, K. Radošević, V. G. Srček, R. N. Das, P. Popelier and K. Roy, *Ecotoxicol. Environ. Saf.*, 2015, **112**, 22-28.
54. V. Kumar and S. V. Malhotra, *Bioorg. Med. Chem. Lett.*, 2009, **19**, 4643.
55. R. J. Bernot, M. A. Brueseke, M. A. Evans-White and G. A. Lamberti, *Environ. Toxicol. Chem.*, 2005, **24**, 87-92.
56. M. T. Garcia, N. Gathergood and P. J. Scammells, *Green. Chem.*, 2005, **7**, 9-14.

57. A. R. Dias, J. Costa-Rodrigues, M. H. Fernandes, R. Ferraz and C. Prudêncio, *ChemMedChem.*, 2017, **12**, 11-18.
58. T. P. Pham, Chul-Woong Cho and Yeoung-Sang Yun, *Water Res.*, 2010, **44**, 352-372.
59. B. Yoo, J. K. Shah, Y. Zhu and E. J. Maginn, *Soft Matter.*, 2014, **10**, 8641-8651.
60. C. G. Cranfield, T. Berry, S. A. Holt, K. R. Hossain, A. P. L. Brun, S. Carne, H. A. Khamici, H. Coster, S. M. Valenzuela and B. Cornell, *Langmuir.*, 2016, **32**, 10725-10734.
61. S. E. Horvath and G. Daum, *Prog. Lipid. Res.*, 2013, **52**, 590-614.
62. S. Fulda, L. Galluzzi and G. Kroemer, *Nat. Rev. Drug Discov.*, 2010, **9**, 447-464.
63. R. Shrestha, E. Johnson and F. L. Byrne, *Mol. Metab.*, 2021, **51**, 101222.
64. T. M. Abdelghany, A. C. Leitch, I. Nevjestic, I. Ibrahim, S. Miwa, C. Wilson, S. Heutz and M. C. Wright, *Food Chem. Toxicol.*, 2020, **145**, 111593.
65. S. Fulda, L. Galluzzi and G. Kroemer, *Nat. Rev. Drug Discov.*, 2010, **9**, 447-464.
66. S. E. Weinberg and N. S. Chandel, *Nat. Chem. Biol.*, 2015, **11**, 9-15.
67. T. M. Ashton, W. G. McKenna, L. A. Kunz-Schughart and G. S. Higgins, *Clin. Cancer Res.*, 2018, **24**, 2482-2490.
68. T. M. Abdelghany, A. C. Leitch, I. Nevjestic, I. Ibrahim, S. Miwa, C. Wilson, S. Heutz and M. C. Wright, *Food Chem. Toxicol.*, 2020, **145**, 111593.
69. F. D. Lofaro, F. Boraldi, M. Garcia-Fernandez, L. Estrella, P. Valdivielso and D. Quaglino, *Front. Cell Dev. Biol.*, 2020, **8**.
70. M. Decler, J. Jovanovic, A. Vakula, B. Udovicki, R. E. K. Agoua, A. Madder, S. De Saeger and A. Rajkovic, *Toxins.*, 2018, **10**.
71. M. D. Brand and D. G. Nicholls, *Biochem J.*, 2011, **435**, 297-312.
72. T. Finkel and N. J. Holbrook, *Nature.*, 2000, **408**, 239-247.
73. J. Ma and X. Li, *Environ. Pollut.*, 2018, **242**, 1337-1345.
74. D. Trachootham, J. Alexandre and P. Huang, *Nat. Rev. Drug Discov.*, 2009, **8**, 579–591.

75. G.-Y. Liou and P. Storz, *Free Radic. Res.*, 2010, **44**, 479-496.
76. P. Korge, S. A. John, G. Calmettes and J. N. Weiss, *J. Biol. Chem.*, 2017, **292**, 9896-9905.